Information Theoretic Bounds for Sensor Network Localization

R. Mudumbai and U. Madhow
Dept. of Electrical and Computer Engineering
University of California, Santa Barbara, CA 93106
Email:raghu@ece.ucsb.edu, madhow@ece.ucsb.edu

***Abstract*— We investigate the fundamental performance limits of target localization, where a network of sensors observe and cooperatively estimate the 2D location of a target. Taking a general view of a sensor as any device whose observations depend statistically on target position, we consider the binary hypothesis testing problem of choosing between the correct target location and an incorrect location at a distance r from it, given the outputs of all sensors in the network. By considering a random placement of sensors in an infinitely large sensing area, we obtain upper and lower bounds on the error probability of this hypothesis testing problem. The error bounds depend only on the type of sensor and are independent of the detailed geometry of the sensor network deployment. This provides a compact comparison of the localization performance of sensors whose characteristics might differ widely (e.g., received signal strength, proximity and time of arrival sensors). Also the bounds decrease exponentially with the density of sensors, and the rate of decrease is shown to have a simple geometric interpretation.**

I. Introduction

We consider the problem of (2D) localization where a network of sensors collaborate to estimate the location of a target within a sensing region. Any device whose observation depends on the target position can be used as a localization sensor. The accuracy of localization depends on the number of sensors available, the geometry of the sensor network, and on the quality of each sensor's observation. For instance localization accuracy can be improved by using a more densely deployed sensor network, or by using less noisy sensors. In this paper we use an information-theoretic approach to quantify this relationship.

We assume a general sensing model where the sensors are specified only by the conditional probability distribution $\Pr(y|\vec{s})$ of the sensor observation y given the location $\vec{s}$ of the sensor relative to the target. Our approach is based on the following simple binary hypothesis testing problem that is related to localization. Given a set of noisy sensor observations, we want to choose between two candidate locations O: the correct target location, and X: a point located distance r away from the correct location. Our key insight is that this problem is analogous to the problem of communicating one of two codewords through a noisy channel; randomizing the sensor placement is equivalent to picking random codewords, and increasing the area of the sensing region is equivalent to increasing the block-length of the codewords. This analogy allows us to use standard information-theoretic techniques to compute bounds on the probability P_r of choosing the error hypothesis X. Furthermore, because of our assumptions of random sensor placement and large sensing region, the bounds are completely independent of the detailed geometry of the sensor network, and thus provide a simple benchmark for comparing the localization accuracy of different types of sensors.

The upper-bound on P_r assumes the simple form $e^{-\lambda A_r}$ where λ is the density of deployment of the sensors, and A_r depends only on $\Pr(y|\vec{s})$. The coefficient A_r has the dimensions of area, and we show that it has a simple geometric interpretation as the *effective coverage area* of a sensor for a desired accuracy r of localization. Intuitively, smaller P_r indicates better localization accuracy.

Related Work. An extensive literature exists on the theory of localization as well as on algorithms for its implementation in sensor networks[1]. This literature is surveyed in [2], and covers a wide range of sensing modalities include RF, acoustic, infrared and video signals, from which various attributes of the target position can be estimated such as range, connectivity, time of arrival (TOA), angle of arrival (AOA) and so on [3], [4]. A virtual radar approach to localization was recently proposed in [5] which uses a combination of TOA and AOA modalities. In [6] it was shown that many of these modalities can be conveniently abstracted as proximity or received signal strength (RSS) observations.

The authors in [6] also analyze the accuracy of localization using the Cramer-Rao bound and by experimental measurements for quantized and unquantized RSS sensors. Specifically it is shown that errors increase with the degree of RSS quantization (as expected from intuition) and are about 50% higher with proximity sensors as compared to unquantized

This work was supported by the National Science Foundation under grants CCF-0431205 and CNS-0520335, by the Office for Naval Research under grant N00014-06-1-0066, and by the Institute for Collaborative Biotechnologies under grant DAAD19-03-D-0004 from the US Army Research Office.

[1]Some of the sensor network literature is concerned with the problem of self-localization, where the sensing nodes cooperatively learn their own position using their observations of each other [1] and a small number of known reference positions or "anchors"; this can be considered as a variation of the target localization problem considered in this paper, and is subject to similar limits on localization accuracy.

RSS sensors. A similar analysis of quantized RSS sensors using the Cramer-Rao bound and simulations is presented in [7]; however the authors in [7] use a different fading model for the RSS and obtain a larger increase in localization error with quantization as compared to [6]. Localization using ideal proximity sensors was studied in [8] using geometric arguments, and it was shown that for a densely deployed network of such sensors the overall localization error is inversely proportional to both the detection range and the sensor density.

In all of these works, the analysis is closely tied to specific types of sensors, and cannot be easily generalized. The authors in [9] propose a Bayesian Bound for the localization error which is simpler to derive compared to the Cramer-Rao bound. Using this bound, the authors show that for TDOA sensors, good localization accuracy can be achieved within the area defined by the convex hull of the sensor locations. The analysis in [9] uses the notion of an optimum sensor observation, defined as the measurement corresponding to a given target position, that would be obtained in the absence of noise. In general this introduces a degree of arbitrariness in identifying the "noise" component of the observation. A hypothesis testing model for localization was first proposed in [10].

Outline. The rest of the paper is organized as follows. In Section II we outline our mathematical model for sensor network localization, and illustrate the model using the examples of proximity, RSS and quantized RSS sensors. We derive upper and lower bounds on the probability of localization error using a Chernoff bound approach in Section III. Some results based on these bounds, specialized to proximity and RSS sensors, are presented in Section IV. Section V concludes with a short discussion of open issues.

II. Mathematical Model for Localization

Consider a target located in a field of N identical sensors. In order to avoid edge effects, we assume a very large sensing area. Without loss of essential generality we take the target position as the origin, and the sensing area $\mathcal{C}_A$ as a circle of radius R_A centered at the origin. Thus $\lambda \doteq \frac{N}{\pi R_A^2}$ is the density of sensors. Each sensor makes a random observation whose distribution depends on the position of the sensor relative to the target. Denoting the position of sensor i by $\vec{s}_i$ and its observation by $y_i \in \mathcal{Y}$, the sensing model is completely specified by the sensing function $f_s(y, \vec{s}) \doteq \Pr(y_i = y | \vec{s}_i = \vec{s})$. Each sensor's observation is conditionally independent of other sensors observations given their locations relative to the target. We denote the outputs of all the N sensors in the network by $\bar{y} \doteq [y_1,\ y_2,\ \ldots,\ y_N]$, and their locations by $\bar{S} \doteq [\vec{s}_1,\ \vec{s}_2,\ \ldots,\ \vec{s}_N]$.

A. Examples of localization sensors

We now introduce two simple sensing models that we will use to illustrate our ideas in the rest of the paper. Both of our examples are *isotropic* sensors whose observations depend only on *distance* from the target and not on its direction i.e. $f_s(y, \vec{s})$ depends only on $|\vec{s}|$. This makes such sensors easier to visualize, however our results in this paper do not require this property and apply to both isotropic and non-isotropic sensors. One important non-isotropic sensor of significant practical importance is the Angle of Arrival (AOA) sensor [11].

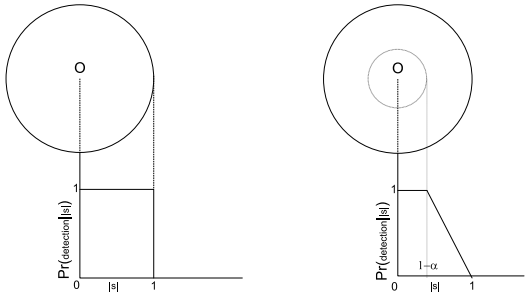

(a) Ideal sensor: always detects a target inside unit circle, and never detects a target outside.

(b) Non-ideal sensor: has a non-zero probability of detection in the annulus.

Fig. 1. Binary proximity sensors.

1) **Binary proximity sensor.** This type of sensor is a detection sensor that outputs a '1' when its observation indicates the presence of a target in its coverage area and a '0' otherwise. This sensor is fully specified by its detection function $f_s(1, s) \equiv Pr(y = 1 || \vec{s}| = s)$.
The *ideal* binary proximity (IBP) sensor always detects a target located within a unit distance i.e. $|\vec{s}| \leq 1$, and never detects a target outside this range. We use this simple sensor extensively in this paper to gain intuition; it plays the same role in our analysis that the error-free binary symmetric channel does for understanding channel capacity. The IBP sensor is illustrated in Fig. 1(a). A non-ideal binary sensor is shown in Fig. 1(b); this sensor always detects a target within a distance $1-\alpha$, never detects a target at a distance greater than 1, but has an "uncertain" region where a target at a distance between $1 - \alpha$ and 1 may be detected with a non-zero probability.
2) **RSS sensor.** This type of sensor measures the received signal strength (RSS) of an incoming signal from the target to estimate distance from the target. For an RF wireless signal, assuming Line of Sight (LoS) transmission the received power varies according to the inverse square law with distance. The sensor observation can be written as
$$y = \left| \frac{A}{|\vec{s}|} + n \right| \tag{1}$$
where n is a (complex) AWGN. According to (1), the sensor observation y follows a Rician distribution. It is possible to modify this model to take into account other impairments such as multi-path and fading effects; however these modifications do not introduce anything conceptually different to the analysis. In this paper we restrict ourselves to the simple RSS sensor given by (1), and the quantized RSS (qRSS) sensor where the observation y is quantized into a finite number of

possible levels. The noiseless outputs of the RSS and qRSS sensors are illustrated in Fig. 2. Note that the binary proximity sensor can be considered as a special case of the qRSS sensor.

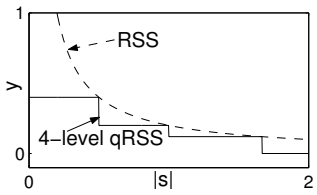

Fig. 2. The observations of an unquantized and a 4-level quantized RSS sensor in the absense of noise plotted against distance $|\vec{s}|$ from target.

III. Bounds for Localization Error

We illustrate the analysis by first considering the special case of the ideal proximity (IBP) sensor. We start with brief review of the following derivation that was originally presented in [8].

A. Localization performance of ideal proximity sensors

When a target is detected by an IBP sensor, it can be inferred that its location is somewhere within the sensor's coverage area i.e. inside a circle of unit radius centered at the sensor's location. Similarly when a target is not detected by an IBP sensor, its location must be somewhere outside of the sensor's coverage area. Given the outputs of all the sensors in the network, we can narrow down the possible locations for the target to a *localization patch* which consists of the intersection of the coverage areas of all detecting sensors, excluding the coverage areas of all non-detecting sensors. In effect the N unit circles representing the coverage areas of the N sensors in the network divide the entire sensing area into a set of localization patches. These patches are illustrated in Fig. 3(a).

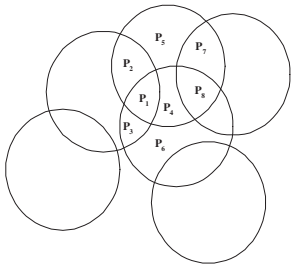

(a) IBP sensors divide the sensing region into localization patches denoted as P_1, P_2 etc.

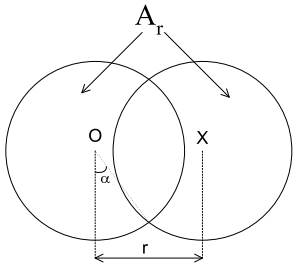

(b) The area A_r represents the set of possible locations for IBP sensors that will result in correct localization of a target at O.

Fig. 3. Localization using ideal binary proximity (IBP) sensors.

The size of the patches determines the localization accuracy of the network. In general the patches can be irregular in shape depending on the sensor placement. If the sensor placement is random, the size of the patch containing the target location (i.e. the origin O) is also random. Consider a point, X located at a distance r from the origin in an arbitrary direction, say the X-axis. The width of the localization patch containing the target is at least as large as r if the same set of sensors detect both O and X. Let us denote this event by $\mathcal{E}_r$ and its probability by P_r. Event $\mathcal{E}_r$ happens if and only if there is no sensor that detects O but not X or vice versa, i.e. there are no sensors in the area A_r in Fig. 3(b).

Under random placement, the number of sensors N_r in A_r follows Poisson statistics with mean λA_r, where we recall λ is the density of sensor deployment. We can now express the probability P_r in terms of the angle[2] $\alpha = \arcsin\left(\frac{r}{2}\right)$ defined in Fig. 3(b):

$$P_r \doteq \Pr(\mathcal{E}_r) \equiv \Pr(N_r = 0) = e^{-\lambda A_r}$$
$$\text{where } A_r = 2\alpha + \sin(2\alpha) \tag{2}$$

Equation (2) can be considered as a lower-bound on the complementary cdf of the width of a localization patch for a network of IBP sensors. However the concept of a localization patch is unique to this type of sensor because its coverage area has a hard boundary. For other types of sensors this definition needs to be generalized. We do this next based on the insight that the random sensor placement considered above is analogous to choosing random code-words for a communication channel.

B. Generalization to arbitrary types of sensors

We first need to generalize the definition of $\mathcal{E}_r$. Given two candidate target locations O and X, we define $\mathcal{E}_r$ as the event that a target located at the origin O is incorrectly localized to X. For the IBP sensor, the sensor observations are deterministic given the sensor positions $\bar{S}$ relative to the target. In a network of IBP sensors, for a given fixed placement of all the sensors, $\Pr(\mathcal{E}_r)$ is either 0 or 1 depending on whether there is at least one sensor in the region A_r in Fig. 3(b) or not. In contrast, the observations of non-IBP sensors are, in general, random (noisy) and we need to specify a decoder. We consider the ML decoder where we choose O if $\Pr(\bar{y}|O,\bar{S}) > \Pr(\bar{y}|X,\bar{S})$, and X otherwise. Note that $P(\bar{y}|O,\bar{S}) = \Pr(\bar{y}|X,\bar{S})$ results in error for this decoder, i.e. $\{\bar{y} : P(\bar{y}|O,\bar{S}) = \Pr(\bar{y}|X,\bar{S})\} \subset \mathcal{E}_r$.

Equation (2) can be interpreted as computing $\Pr(\mathcal{E}_r)$ for a large number of fixed placements $\bar{S}$ and then taking an average. With this interpretation we can extend the analysis of Section III-A to arbitrary types of sensors. Since the sensor outputs are conditionally independent of each other, we have

$$\Pr(\bar{y}|O,\bar{S}) = \prod_{i=1}^{N} \Pr(y_i|O,\vec{s}_i) = \prod_{i=1}^{N} f_s(y_i,\vec{s}_i)$$
$$\Pr(\bar{y}|X,\bar{S}) = \prod_{i=1}^{N} \Pr(y_i|X,\vec{s}_i) = \prod_{i=1}^{N} f_s\big(y_i,(\vec{s}_i-\vec{x})\big) \tag{3}$$

[2]The angle α is undefined when the two circles in Fig. 3(b) do not intersect i.e. when $r > 2$. To be consistent with later results, we simply define α to be 90° for $r > 2$.

where $\vec{x}$ represents the position X. We define the following disjoint "decoding sets":

$$\begin{aligned}\mathcal{D}_O &\doteq \{\bar{y} : \Pr(\bar{y}|O,\bar{S}) > \Pr(\bar{y}|X,\bar{S})\}\\ \mathcal{D}_X &\doteq \{\bar{y} : \Pr(\bar{y}|O,\bar{S}) < \Pr(\bar{y}|X,\bar{S})\}\\ \mathcal{D}_{XO} &\doteq \{\bar{y} : \Pr(\bar{y}|O,\bar{S}) = \Pr(\bar{y}|X,\bar{S})\}\end{aligned} \tag{4}$$

We also define the error probabilities

$$\begin{aligned}P_{e|O,\bar{S}} &\doteq \Pr\left((\mathcal{D}_X \cup \mathcal{D}_{XO})\middle|O,\bar{S}\right)\\ P_{e|X,\bar{S}} &\doteq \Pr\left((\mathcal{D}_O \cup \mathcal{D}_{XO})\middle|X,\bar{S}\right)\end{aligned} \tag{5}$$

Then we have

$$P_r \equiv \Pr(\mathcal{E}_r) = \mathsf{E}_{\bar{S}}\left[P_{e|O,\bar{S}}\right] \tag{6}$$

Using standard Chernoff bounding techniques ([12], pp.121), we can upper-bound $P_{e|O,\bar{S}}$ as

$$P_{e|O,\bar{S}} \le \int_{\bar{y}\in\mathcal{Y}^N} \Pr(\bar{y}|O,\bar{S})^{1-\gamma}\Pr(\bar{y}|X,\bar{S})^{\gamma}\, d\bar{y} \tag{7}$$

for[3] any non-negative γ. With $\gamma = 0.5$, we also have the following lower-bound ([12], pp.127)

$$P_{e|O,\bar{S}} + P_{e|X,\bar{S}} \ge \frac{1}{2}\left(\int_{\bar{y}} \sqrt{\Pr(\bar{y}|O,\bar{S})\Pr(\bar{y}|X,\bar{S})}\, d\bar{y}\right)^2 \tag{8}$$

We can now use the conditional independence of the sensor observations to simplify these expressions. Using (3) in (7) we have

$$P_{e|O,\bar{S}} \le \prod_{i=1}^{N}\left(\int_{y_i\in\mathcal{Y}} f_s(y_i,\vec{s}_i)^{1-\gamma} f_s\big(y_i,(\vec{s}_i-\vec{x})\big)^{\gamma}\, dy_i\right)$$

Noting that y_i is just a dummy variable of integration, we have

$$\begin{aligned}P_{e|O,\bar{S}} &\le \prod_{i=1}^{N}\big(1 - f_r(\vec{s}_i,\gamma)\big),\ \forall\gamma \ge 0\\ f_r(\vec{s},\gamma) &\doteq 1 - \int_{y\in\mathcal{Y}} f_s(y,\vec{s})^{1-\gamma} f_s\big(y,(\vec{s}-\vec{x})\big)^{\gamma}\, dy\end{aligned} \tag{9}$$

By definition $f_r(\vec{s},\gamma) \le 1$ with equality if and only if the support sets of $f_s(y,\vec{s})$ and $f_s\big(y,(\vec{s}-\vec{x})\big)$ do not overlap (except for a zero probability subset of $\mathcal{Y}$). Further for $\gamma \le 1$, we have using Jensen's Inequality that

$$f_s(y,\vec{s})^{1-\gamma} f_s\big(y,(\vec{s}-\vec{x})\big)^{\gamma} \le (1-\gamma) f_s(y,\vec{s}) + \gamma f_s(y,(\vec{s}-\vec{x}))$$

Therefore $f_r(\vec{s},\gamma) \ge 0$ with equality if and only if $f_s(y,\vec{s}) = f_s\big(y,(\vec{s}-\vec{x})\big)$ for almost all $y \in \mathcal{Y}$.

Note that an IBP sensor located *inside* the region labeled A_r in Fig. 3(b) satisfies $f_r(\vec{s},\gamma) = 1$, and an IBP sensor located *outside* A_r satisfies $f_r(\vec{s},\gamma) = 0$.

These observations lead to the intuitive interpretation of $f_r(\vec{s},\gamma)$ as the probability that a sensor located at $\vec{s}$ can successfully disambiguate a target at the origin O from a target at location X. Fig. 4 shows mesh plots of $f_r(\vec{s},\gamma)$ with

[3]If the set of sensor observations $\mathcal{Y}$ is discrete, all integrals over $\mathcal{Y}$ should be replaced by summations.

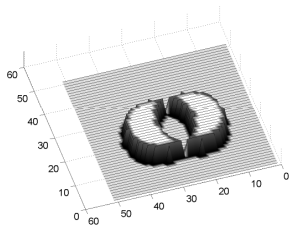

(a) IBP sensor.

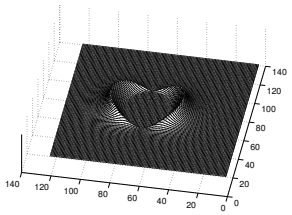

(b) 4-level qRSS sensor, noise variance $E[|n|^2] = 0.1$.

Fig. 4. 3D mesh plot of $f_r(\vec{s},\gamma)$ as a function of sensor location $\vec{s}$ with $\gamma = 0.5$ and $r = 1$; the volume under this plot is equal to A_r.

$\gamma = 0.5$ for a IBP sensor and a 4-level qRSS sensor with a small noise variance. We note the resemblance of Fig. 4(a) to the region A_r in Fig. 3(b); specifically we see that the exponent A_r of the localization error probability given by (2) is equal to the volume under the mesh of $f_r(\vec{s},\gamma)$ for the IBP sensor. We now show that the same relationship holds for any type of sensor.

C. Averaging over random sensor placements

We now bound P_r using (6), by averaging (7) and (8) over randomized sensor placements $\bar{S}$; each sensor is placed independently at a randomly chosen position in the sensing region, $\mathcal{C}_A$ i.e. a circle of radius $R_A \gg 1$ centered at the origin. Using (9) in (7), we have

$$\begin{aligned}P_r &\le \mathsf{E}_{\bar{S}}\left[\prod_{i=1}^{N}\big(1 - f_r(\vec{s}_i,\gamma)\big)\right] = \prod_{i=1}^{N}\mathsf{E}_{\vec{s}_i}\big[1 - f_r(\vec{s}_i,\gamma)\big]\\ &= \big(1 - \mathsf{E}_{\vec{s}}\big[f_r(\vec{s},\gamma)\big]\big)^N,\ \forall\gamma \ge 0\end{aligned} \tag{10}$$

If $dA(\vec{s})$ is an infinitesimal area element at position $\vec{s}$, the probability that a given sensor will be placed within that area is $\frac{dA(\vec{s})}{\pi R_A^2}$. Thus we have

$$\begin{aligned}&\mathsf{E}_{\vec{s}}\big[f_r(\vec{s},\gamma)\big] \le \frac{A_r}{\pi R_A^2},\ \text{where } A_r \doteq \max_{\gamma\ge 0} A_r(\gamma),\\ &\text{and } A_r(\gamma) \doteq \int_{\vec{s}\in\mathcal{C}_A} f_r(\vec{s},\gamma)\, dA(\vec{s})\end{aligned} \tag{11}$$

As R_A becomes large, we expect $\frac{A_r}{\pi R_A^2} \to 0$, because under any reasonable sensing model, the contribution of far-away sensors decreases with distance from the target. Using (11) and $N = \lambda\pi R_A^2$ in (10), we get in the limit of large R_A

$$P_r \le \lim_{R_A\to\infty}\left(1 - \frac{A_r}{\pi R_A^2}\right)^{\lambda\pi R_A^2} \equiv e^{-\lambda A_r} \tag{12}$$

When the sensing area $\mathcal{C}_A$ is large, there is a symmetry between O and X, and we can show that $A_r(\gamma) \equiv A_r(1-\gamma),\ \forall\gamma \in (0,1)$. Furthermore we can show that $\gamma = 0.5$ maximizes $A_r(\gamma)$, and A_r is simply the *Bhattacharya bound* given by

$$A_r \equiv \int_{\vec{s}}\int_{y}\left(\sqrt{f_s(y,\vec{s})f_s\big(y,(\vec{s}-\vec{x})\big)}\right) dy\ dA(\vec{s}) \tag{13}$$

The symmetry between O and X also gives $E_{\bar{S}}[P_{e|O,\bar{S}}] \equiv E_{\bar{S}}[P_{e|X,\bar{S}}]$. Therefore we have from (8)

$$P_r \geq \frac{1}{4} E_{\bar{S}} \left[\Big(\int_{\bar{y}} \sqrt{\Pr(\bar{y}|O,\bar{S}) \Pr(\bar{y}|X,\bar{S})}\ d\bar{y} \Big)^2 \right]$$
$$\geq \frac{1}{4} \left(E_{\bar{S}} \big[\int_{\bar{y}} \sqrt{\Pr(\bar{y}|O,\bar{S}) \Pr(\bar{y}|X,\bar{S})}\ d\bar{y} \big] \right)^2$$

where we used the Jensen's Inequality for $E[(.)^2] \geq (E[.])^2$. Thus we have both upper and lower bounds for P_r in terms of A_r:

$$\frac{1}{4} e^{-2\lambda A_r} \leq P_r \leq e^{-\lambda A_r} \tag{14}$$

As noted earlier, for the IBP sensor, A_r is equal to the area of the region labeled A_r in Fig. 3(b), and (12) reduces to (2). This suggests that we can think of A_r as the *effective coverage area* of a sensor; roughly speaking it corresponds to the area where the sensor's observations can successfully localize a target to within an error of r.

IV. Numerical Results

We now look at some numerical results to further build intuition into the bound (12). Fig. 5(a) shows a plot of A_r for the binary proximity sensors of Fig. 1. The figure shows that as the width α of the uncertain sensing region decreases, the coverage area of the non-ideal binary sensor approaches that of the IBP sensor as given by (2).

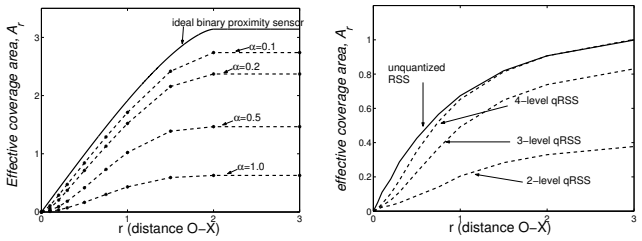

(a) Ideal and non-ideal binary proximity sensors.

(b) Quantized and unquantized RSS sensors.

Fig. 5. The "effective coverage area" A_r of BPS and RSS sensors.

Fig. 5(b) shows A_r for quantized and unquantized RSS sensors. The measurement model follows (1) with the transmit power and noise variance normalized to unity, i.e. $A = 1$ and $\mathsf{E}\big[|n|^2\big] = 1$. No attempt was made to optimize the RSS quantization levels, which were simply chosen as $\mathcal{Y} = \{0,1\},\ \mathcal{Y} = \{0,1,2\},\ \mathcal{Y} = \{0,1,2,3\}$ for the three qRSS sensors shown. Clearly the 2-level qRSS sensor is highly suboptimal compared to the 4-level sensor, whose performance is close to the unquantized sensor except for very small r.

V. Conclusion

The main contribution of this paper is the derivation of upper and lower bounds on the probability, P_r of incorrect localization with random sensor placement. This bound depends only on the sensing characteristic and not on the details of specific deployments such as the size of the network and the sensor locations. Thus it provides an objective metric to compare the localization accuracy of different types of sensors.

Our analysis of localization error is based on a hypothesis testing problem which involves choosing between two candidate target locations based on the sensor observations. More generally, localization is the parameter estimation problem of computing an estimate of the (2D) target location, rather than choosing from a finite number of candidate locations. When the density of deployment λ is very large, we expect that the likelihood function is highly peaked close to the origin, and since P_r is the probability that the likelihood of location X is larger than at the origin, we expect it provides a good lower-bound to the complementary cdf of the localization error of a ML estimator i.e. $\Pr(|\vec{x}_{ML}| > r) \gtrapprox P_r$. A detailed exploration of this relationship is beyond our scope here, and is an important open issue for future work.

Other open problems include an enquiry into the general properties of "effective coverage area" A_r; for instance we would expect A_r to be monotonically non-decreasing in r for most sensors.

References

[1] R. Moses, D. Krishnamurthy, and R. Patterson, "Self-localization for wireless networks," *Eurasip J. Appl. Signal Process.*, pp. 348–358, 2003.

[2] N. Patwari, J. N. Ash, S. Kyperountas, A. O. Hero, R. L. Moses, and N. S. Correal, "Locating the nodes: cooperative localization in wireless sensor networks," *IEEE Signal Processing Magazine*, vol. 22, no. 4, pp. 54–69, July 2005.

[3] D. Moore, J. Leonard, D. Rus, and S. Teller, "Robust distributed network localization with noisy range measurements," in *SenSys '04: Proceedings of the 2nd international conference on Embedded networked sensor systems*, 2004, pp. 50–61.

[4] T. He, C. Huang, B. M. Blum, J. A. Stankovic, and T. Abdelzaher, "Range-free localization schemes for large scale sensor networks," in *MobiCom '03: Proceedings of the 9th annual international conference on Mobile computing and networking*, 2003, pp. 81–95.

[5] B. Ananthasubramaniam and U. Madhow, "On localization performance in imaging sensor nets," *IEEE Trans. Signal Processing*, vol. 55, no. 10, pp. 5044–5057, Oct 2007.

[6] N. Patwari and A. O. Hero, "Using proximity and quantized RSS for sensor localization in wireless networks," in *WSNA '03: Proceedings of the 2nd ACM international conference on Wireless sensor networks and applications*, 2003, pp. 20–29.

[7] H. Shi, X. Li, Y. Shang, and D. Ma, "Cramer-Rao Bound Analysis of Quantized RSSI Based Localization in Wireless Sensor Networks," *11th International Conference on Parallel and Distributed Systems (ICPADS'05)*, vol. 02, pp. 32–36, 2005.

[8] N. Shrivastava, R. Mudumbai, U. Madhow, and S. Suri, "Target tracking with binary proximity sensors: fundamental limits, minimal descriptions, and algorithms," in *SenSys '06: Proceedings of the 4th international conference on Embedded networked sensor systems*, 2006, pp. 251–264.

[9] H. Wang, L. Yip, K. Yao, and D. Estrin, "Lower bounds of localization uncertainty in sensor networks," *Proc. IEEE Intl. Conf. on Acoustics, Speech, and Signal Process. (ICASSP '04)*, vol. 3, pp. iii–917–20, May 2004.

[10] S. Ray, W. Lai, and I. C. Paschalidis, "Statistical location detection with sensor networks," *IEEE Transactions on Information Theory*, vol. 52, no. 6, pp. 2670–2683, June 2006.

[11] P. Rong and M. L. Sichitiu, "Angle of arrival localization for wireless sensor networks," *3rd Annual IEEE Communications Society on Sensor and Ad Hoc Communications and Networks SECON '06*, vol. 1, pp. 374–382, Sept 2006.

[12] H. V. Poor, *An Introduction to Signal Detection and Estimation*. Springer-Verlag, 1988.